Earthquakes and Structures, Vol. 3, No. 5 (2012) 629-647
DOI: http://dx.doi.org/10.12989/eas.2012.3.5.629

Characterization of earthquake ground motion of multiple sequences

Abbas Moustafa*[1] and Izuru Takewaki[2]

[1]Department of Civil Engineering, Minia University, Minia 61111, Egypt
[2]Dept. of Architecture & Architectural Engineering, Kyoto University, Kyotodaigaku-Katsura, Kyoto, 615-8540, Japan

(Received March 7, 2011, Revised November 25, 2011, Accepted December 9, 2011)

Abstract. Multiple acceleration sequences of earthquake ground motions have been observed in many regions of the world. Such ground motions can cause large damage to the structures due to accumulation of inelastic deformation from the repeated sequences. The dynamic analysis of inelastic structures under repeated acceleration sequences generated from simulated and recorded accelerograms without sequences has been recently studied. However, the characteristics of recorded earthquake ground motions of multiple sequences have not been studied yet. This paper investigates the gross characteristics of earthquake records of multiple sequences from an engineering perspective. The definition of the effective number of acceleration sequences of the ground shaking is introduced. The implication of the acceleration sequences on the structural response and damage of inelastic structures is also studied. A set of sixty accelerograms is used to demonstrate the general properties of repeated acceleration sequences and to investigate the associated structural inelastic response.

Keywords: ground motion; acceleration sequences; inelastic structures; damage index

1. Introduction

Ground-motion sequences separated by short time-intervals have been observed in several parts of the world including Japan, Mexico, Turkey, Italy, Peru and California. This data, however, is not available in a data base for easy access to structural engineers. Such ground motion sequences can cause significant damage to the structures due to accumulation of the inelastic deformation from the repeated sequences before any repair is possible. Moreover, the low-frequency content in the secondary sequences may cause resonance in lower modes of the damaged structure leading to further damage. The verification of the structure capacity to withstand multiple acceleration sequences without collapse is of great importance, especially since current seismic codes do not account for their effects.

Elnashai *et al*. (1998) shed the light on this subject and reported significant increase in the strength demand of ductile structures to multiple acceleration sequences. The dynamic analysis of inelastic structures under acceleration sequences has been studied by a few authors (Amadio *et al.* 2003, Das *et al.* 2007). Numerically simulated acceleration sequences have been used as input to

*Corresponding author, Associate Professor, E-mail: abbas.moustafa@mu.edu.eg

inelastic structures. Extensive investigations on the displacement ratio of single-degree-of-freedom (SDOF) inelastic structures under repeated earthquakes have been carried out recently by Hatzigeorgiou and Beskos (2009). 112 ordinary accelerograms recorded at four different soil sites have been used to produce two and three repeated sequences. More recently, Hatzigeorgiou (2010a,b) studied near-fault and far-fault repeated acceleration sequences using ordinary recorded accelerograms for different soil types and derived analytical expressions for the inelastic displacement ratio and the ductility demand in terms of the period of vibration, the viscous damping ratio, the strain-hardening ratio, the force reduction factor and the soil class. Although most research carried out so far has focused on the effect of the repeated earthquake shakings on SDOF systems, there has been some work also on multi-degree-of-freedom (MDOF) systems (Nour *et al*. 1992, Fragiacomo *et al*. 2004, Li and Ellingwood 2007). These studies have shown that repeated acceleration sequences can produce large deformations in the structures. Notwithstanding this, the characteristics of recorded earthquakes of multiple sequences have not been studied yet.

Given the enormous growth in strong ground-motion data worldwide over the last 76 years, it is of interest to investigate the general characteristics of repeated acceleration sequences from an engineering perspective. This aspect is of relevance to (a) the mathematical modeling and simulation of ground motion sequences, (b) the selection of earthquake records as input to the time-history analysis of inelastic structures and (c) the performance-based seismic design of the structures. The objectives of this paper are to investigate: (1) the general characteristics of strong ground motion sequences using actual recorded data and (2) the associated response of inelastic structures.

Finally, this study aims to emphasize the need for considering repeated acceleration sequences in seismic design of the structures. In this context, it may be recalled that, the 1994 Northridge and the 1995 Hyogoken-Nanbu earthquakes have motivated modern seismic codes to introduce modification factors to the design spectra of near-fault regions (ECS 2003, Bray and Rodriguez-Marek 2004, AIJ 2005, Krawinkler *et al*. 2005, Kalkan and Kunnath 2006, IBC 2009). The purpose of this paper is not to identify whether multiple sequences are components of a series of main shock-foreshock-aftershock events of the same event or to provide statistical analyses for the parameters of the repeated acceleration sequences, but to demonstrate their general feature from an engineering perspective and to provide a guide for the seismic load/demand for inelastic structures under multiple sequences. The characteristics of recorded sequences are studied in the next section.

2. Characteristics of earthquake records of multiple sequences

2.1 General features of recorded accelerations

The two horizontal and the vertical accelerations of a set of 54 strong-motion accelerograms from 18 earthquakes recorded in seven countries are considered herein. Table 1 summarizes information on these records. This information includes the moment magnitude, the observed number of sequences, the site-source distance, the total duration, the peak ground acceleration (PGA) and the Arias intensity (square root of the area under the square of the ground acceleration) (Arias 1970). The earthquake date, time of occurrence, the site, the recording station and the local soil condition beneath the recording station are also included in the table. The digitized accelerations data has been accessed from the COSMOS database Center (COSMOS 2009), the Kyoshin-Network (K-Net 2009),

Table 1 Information on strong ground-motions with multiple acceleration sequences

Earthquake	Date	Time	Soil type	Site (station)	N_s	M	D_{ss} (km)	t_d (s)	PGA (g)			E (m/s$^{3/2}$)		
									H_1	H_2	UD	H_1	H_2	UD
Helena aftershock	11.28.1935	14:41:48	Rock	Helena Federal Bldg (HFB)	2	5.0	6.3	45	0.09	0.08	0.03	1.47	1.76	0.58
San Francisco	03.22.1957	19:44:21	Alluvium	350 McAllister (USGS1080)	2	5.3	17.0	41	0.10	0.07	0.05	0.64	0.47	0.44
San Fernando	02.09.1971	14:02:24	Rock	Pacoima dam (CSMIP24207)	2	3.9	10.9	31	0.12	0.13	0.05	0.70	0.57	0.29
Victoria	06.09.1980	03:28:19	Alluvium	Chihuahua, Mexico (6621)	2	6.4	5.7	56	0.19	0.15	0.17	1.89	1.77	1.13
New Zealand	06.18.1994	03.25.15	medium	Arthurs Pass (GNS505A)	3	6.8	16.0	160	0.44	0.34	0.37	5.49	3.47	3.24
Katsurao	02.20.1997	05:22:00	Soft soil	Katsurao (FKS006)	2	5.3	39.0	67	0.12	0.12	0.06	0.87	0.86	0.45
Kocaeli	08.17.1999	00:01:40	Soft soil	Yarimca (KOER772)	2	7.4	22.7	136	0.23	0.32	0.24	3.14	3.17	2.74
Chi-Chi	09.20.1999	17:47:16	Stiff soil	Taichung (TCU071)	2	7.6	4.9	160	0.53	0.65	0.42	6.30	9.62	5.06
Chi-Chi	09.20.1999	18:03:00	Stiff soil	Taichung (TCU078)	2	6.2	7.6	65	0.28	0.47	0.24	2.28	3.66	1.20
Bhuj	01.26.2001	03:16:40	NA	Ahmd abad (IITR)	2*	7.0	239.0	134	0.11	0.08	0.07	1.31	1.01	0.80
Niigata	10.23.2004	17:56:00	Soft soil	Ojiya (NIG019)	2	6.8	7.0	299	1.17	1.33	0.84	9.83	11.64	6.97
Niigata	10.23.2004	17:56:00	NA	Nagaoka-shisho (NIG028)	2	6.8	15.0	580	0.89	0.72	0.44	9.70	7.84	4.72
Niigata	10.23.2004	18:03:00	Soft soil	Ojiya (NIG019)	2**	6.3	18.0	299	0.20	0.23	0.10	1.95	2.40	1.03
Niigata	10.23.2004	18.07:00	Soft soil	Koide (NIG020)	3	5.7	15.0	299	0.12	0.12	0.04	0.76	0.76	0.36
Niigata	10.23.2004	18:34:00	Soft soil	Koide (NIG020)	2	6.5	09.0	299	0.54	0.53	0.34	5.65	4.07	2.51
Niigata	10.23.2004	19:46:00	Soft soil	Koide (NIG020)	3	5.7	10.0	299	0.15	0.13	0.06	1.23	1.15	0.61
Niigata	10.27.2004	10:40:00	Soft soil	Koide (NIG020)	2	6.1	9.0	299	0.53	0.40	0.54	3.51	2.53	2.16
Honshu	04.15.2007	19:47:00	Soft soil	Kohga (SIG012)	2	5.4	13.0	120	0.26	0.11	0.05	2.05	0.53	0.41
Niigata-ken	08.16.2007	04:15:00	Soft soil	Hasunuma (CHBH19)	2	5.3	17.0	147	0.10	0.03	0.04	0.55	0.42	0.27
Iwate-Miyagi	06.14.2008	09:20:00	Soft soil	Ichinoseeki-w (IWTH25)	2	5.7	22.0	212	0.80	0.21	0.47	2.61	1.20	1.73
El Centro***	05.19.1940	04:37:00	Soft soil	117 El Centro array # 9	0	7.0	12.99	40	0.22	0.31	0.21	3.27	3.57	1.79
Hyogoken-Nanbu***	01.16.1995	20:46:00	NA	Kobe University	0	6.9	0.90	32	0.31	0.29	0.38	2.26	2.76	2.03

NA = not available, N_s = Number of acceleration sequences, M = Magnitude, D_{ss} = Site-source distance, t_d = total duration, *UD component only has two acceleration sequences, **UD component has five acceleration sequences, ***ordinary records without acceleration sequences, H_1 = first horizontal acceleration component, H_2 = second horizontal acceleration component, UD = vertical acceleration component.

the Kiban Kyoshin-Network (KiK-Net 2009), and the Pacific Earthquake Engineering Research (PEER) Center (PEER 2009). These records cover a variety of earthquake magnitude, duration, soil condition, site-source distance and peak ground acceleration. Note that, these records represent strong ground motion ($M \geq 5.0$ or PGA ≥ 0.05 g). The selection criterion of these records was not based on the site-source distance, the duration or the soil class. Given the limited number of records used in this study, this paper aims to emphasize the gross features of strong ground motion of multiple-sequences from an engineering perspective and to investigate the associated structural inelastic response. The paper does not focus on the seismological aspects of multiple-acceleration sequences or on characterizing the earthquake properties quantitatively which requires a large number of earthquake records and additional information on the source properties.

Table 1 contains also information on the three acceleration components of two ordinary earthquakes without sequences. Namely, the 1940 Imperial Valley (El Centro) earthquake recorded at El Centro array #9 and the 1995 Hyogoken-Nanbu (Kobe) earthquake recorded at the Kobe university recording station are considered for comparison. Fig. 1 shows the three acceleration components for earthquakes having two and three sequences (see Table 1). Based on a careful investigation of these records, the following observations are made:

1. Source-site distance: Most records except Katsurao and Bhuj earthquakes represent strong ground motion measured at the near-fault region with site-source distance less than about 23 km. The three records of each earthquake contain distinct sequences. The sequence trend is also observable in the velocity and the displacement. The acceleration records of the Katsurao earthquake (site-source distance = 39 km) have two sequences. The vertical acceleration only of Bhuj earthquake contains two sequences which could be attributed to the local soil effects (COSMOS 2009).
2. Influence of source mechanism: Some records of repeated sequences are measured at sites with soil conditions while other records are reported at sites with rock condition. This implies that the occurrence of repeated acceleration sequences is independent of the local soil condition beneath the recording station. Thus, such ground motion is primarily influenced by the source mechanism where the energy flow at the source is released in sequences separated by short-intervals of time.
3. Number of acceleration sequences: The observed number of acceleration sequences is generally two or three (see Table 1 and Fig. 1). A larger number of sequences have been observed in a few records. For example, the vertical acceleration of the 2004 Niigata earthquake recorded at Ojiya (NIG019) contains five sequences (see Table 1). Note that, the number of acceleration sequences depends on the records considered and thus it may change if a large number of records are used. Note also that, a criterion for defining the effective number of acceleration sequences does not exist, and is introduced in the next section.
4. Total duration and duration of individual sequences: The total duration for the records listed in Table 1 is substantially larger than those of ordinary records, and, ranges between about 1.0 and 10.0 minutes. Some records, however, have shorter durations than 1.0 minute (see Table 1). The duration of individual sequences (duration between 5% and 95% of the sequence energy) is significantly small (typically about 5-30 s) (Trifunac and Brady 1975). The individual sequences of most records have sharp build up, short strong-phase and sudden decay. The time-intervals separating the acceleration sequences are about 1-3 times the duration of the individual sequences. Note that the earthquake total duration will automatically change if the number of records is increased.

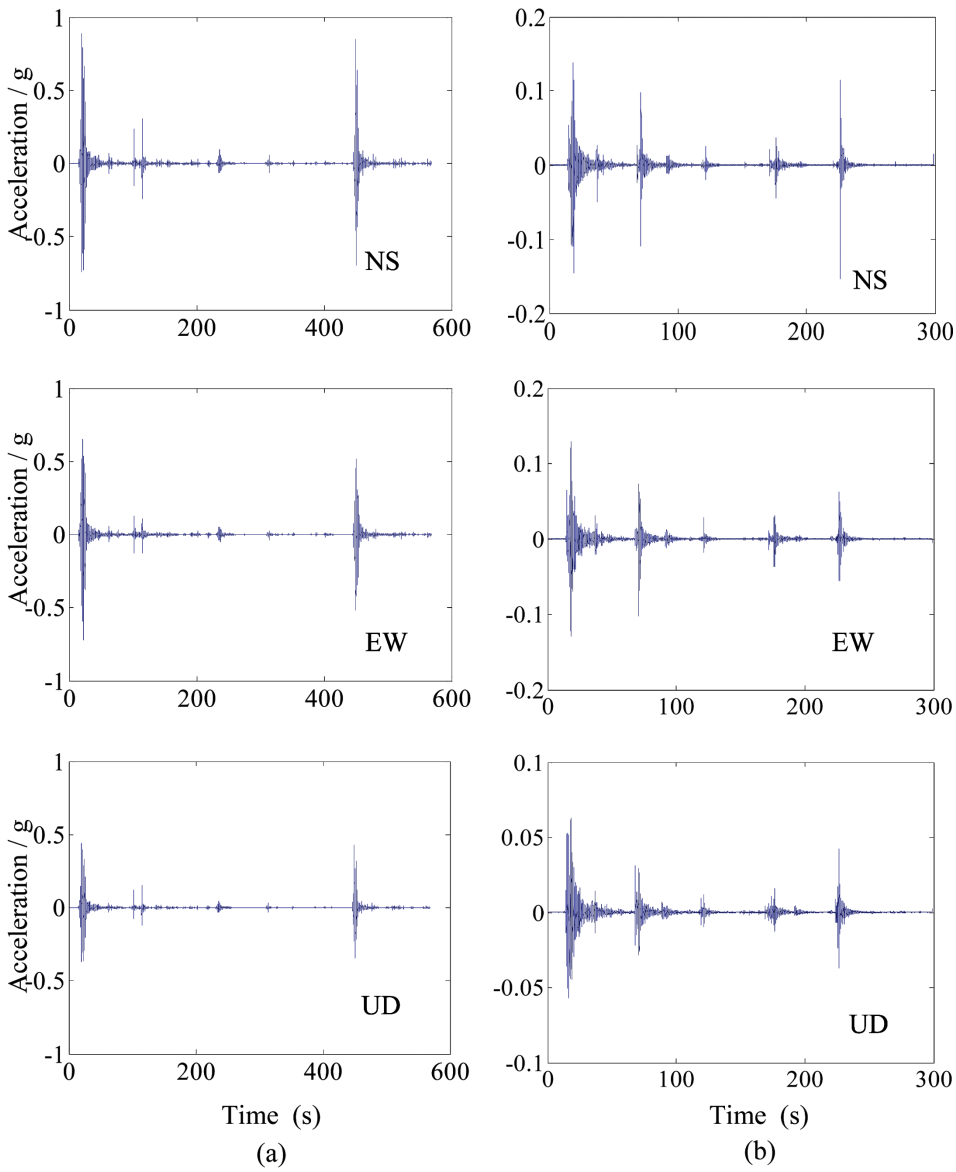

Fig. 1 Ground accelerations with multiple sequences: (a) 2004 Niigata earthquake at Nagaoka-shisho (NIG028) and (b) 2004 Niigata earthquake at Koide (NIG020)

5. Frequency content of individual sequences: Fig. 2 shows the Fourier amplitude spectra for each sequence for the NS acceleration components of the 2004 Niigata and the 2007 Honshu earthquakes (see Table 1). These plots reveal that the frequency content and the amplitude for the individual sequences of the same record could be significantly different. Hence, in simulating repeated acceleration sequences, the consideration of identical sequences may not be accurate.
6. Distribution of energy in sequences: In general, the individual sequences of the same record have different energies and durations. Additionally, the individual sequences have sharp build

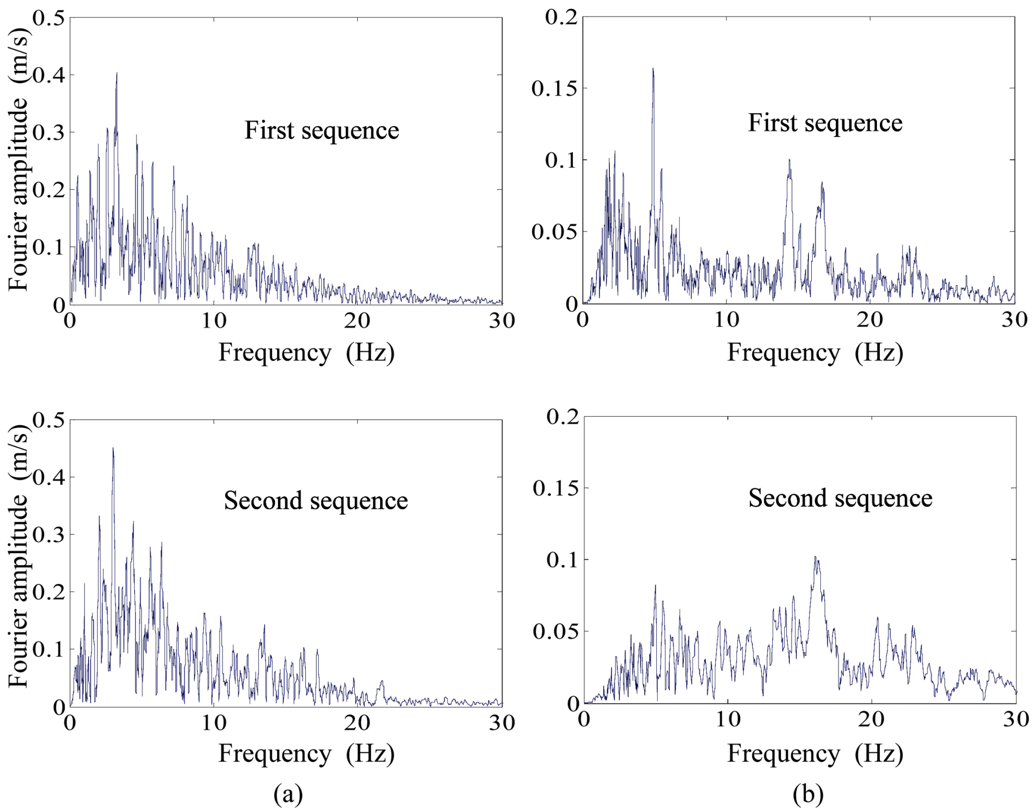

Fig. 2 Fourier amplitude spectra for individual sequences: (a) 2004 Niigata (NIG028-NS) and (b) 2007 Honshu (SIG012-NS)

up of energy (see Figs. 3 and 4).

7. Peak ground acceleration: The peak ground acceleration is generally contained in the first sequence and the largest observed PGA is 1.33 g. In this study, we limited our attention to ground motions with minimum PGA of about 0.05 g. Some records, however, have PGA slightly less than 0.05 g but $M \geq 5.0$.
8. Magnitude range: The earthquake magnitude for the ground motions reported in this paper ranges between 5.0 and 7.4 (see Table 1). One earthquake, however, has magnitude = 3.9, but the associated peak ground accelerations are larger than 0.05 g.
9. Correlation of acceleration components: The three acceleration components of each earthquake exhibit significant correlations (see Fig. 1). The corresponding sequences in the three records of the same earthquake have similar durations and time instants of initial build up, strong-phase and decay. As can be expected, the cross-correlation functions of the acceleration components are significant during the strong shaking durations (see Fig. 5).

It may be noted that the total duration and the associated effective number of sequences for ground accelerations of multiple sequences depend primarily on the selected records. The duration of the record may depend on the triggering mechanism of the instruments, on the protocol that each agency uses for data storage, and on the ground motion processing methodology. This implies that there may be more records with multiple sequences than those reported in this study. Moreover, if

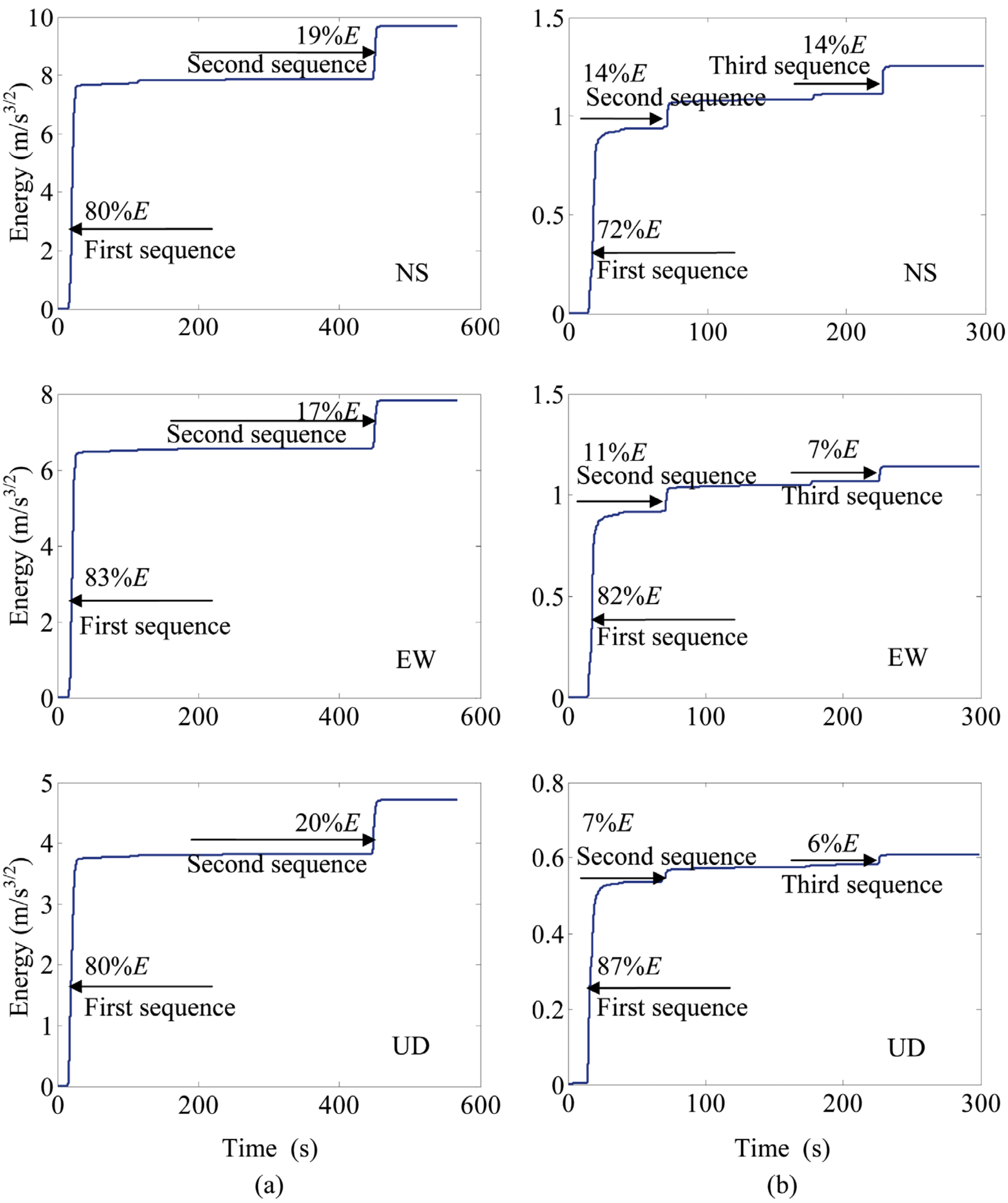

Fig. 3 Time-variation of energy for acceleration sequences estimated from Eq. (1): (a) 2004 Niigata at Nagaoka-shisho (NIG028) and (b) 2004 (19:46:00) Niigata at Koide (NIG020)

additional records are used, the reported total duration and effective number of sequences may change. It should be emphasized, however, that this paper does not provide statistical analyses for these parameters but focuses on the gross features of repeated acceleration sequences using actual recorded ground motion sequences and on the associated structural inelastic response. Furthermore, this section describes the gross features of repeated acceleration sequences from an engineering perspective. The seismological properties of repeated acceleration sequences require further

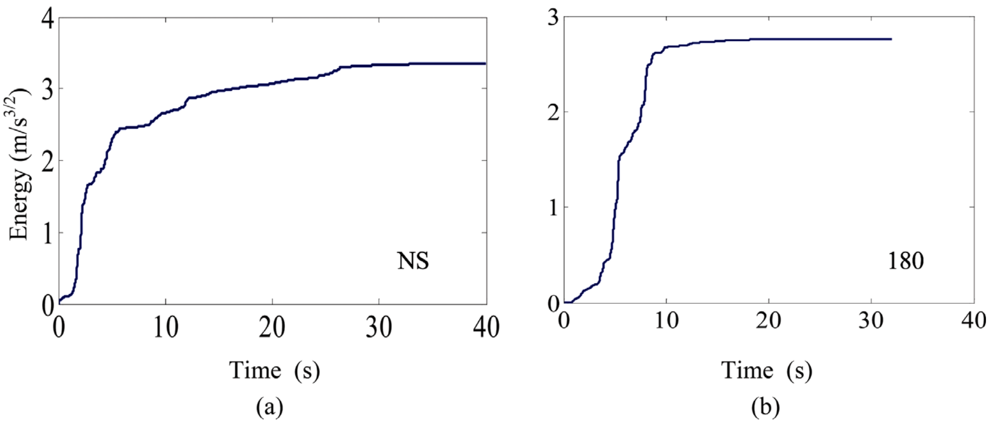

Fig. 4 Time-variation of energy for ordinary earthquakes: (a) 1940 Imperial valley earthquake (El Centro array #9) and (b) 1995 Hyogoken-Nanbu earthquake (Kobe University)

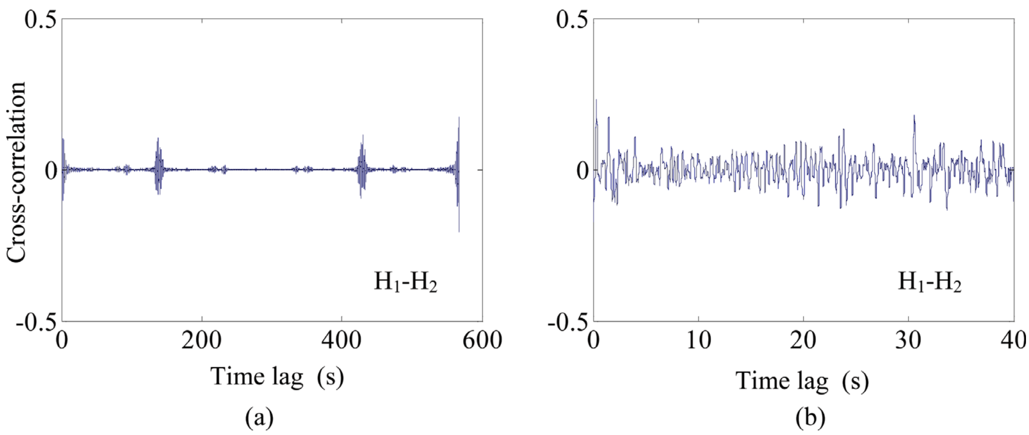

Fig. 5 Cross-correlation functions of ground accelerations: (a) 2004 Niigata earthquake (NIG028) and (b) 1940 El Centro (El Centro #9)

information on the source properties and can be studied in a separate paper.

The next section investigates the energy, frequency content and effective number of sequences and effective duration of repeated acceleration sequences.

2.2 Specific characteristics of recorded accelerations

In this section we examine the time variation of the energy of strong ground-motion of repeated sequences. The definition of the effective number of sequences is also introduced. The acceleration energy is defined in terms of the Arias intensity as follows (Arias 1970)

$$E(t) = \left[\int_0^t [\ddot{x}(\tau)]^2 d\tau \right]^{1/2} \tag{1}$$

where $\ddot{x}(t)$ is the ground acceleration, and τ is a dummy time variable. The total energy is estimated by replacing t with t_d (t_d = total duration) in the above equation.

Fig. 3 depicts the time variation of energy estimated using Eq. (1) for the three acceleration components for the earthquake records shown in Fig. 1. Fig. 4 shows the energy for one of the horizontal accelerations (H_1 in Table 1) for the two ordinary earthquakes without sequences. The multiple sequences have repeated build up of energy during each sequence and no significant contribution from the time-intervals separating sequences. This feature is more remarkable in the Niigata accelerograms recorded at Nagaoka-shisho (Fig. 3(a)). The contribution to the total energy from the first sequence is remarkably high (72-87%) while that from the secondary sequences is small (6-20%). Note that, minor secondary sequences of low amplitude exist in some records. These sequences have small build up of energy (Fig. 3(b)). The contribution from these secondary sequences to the total energy is very small. We use this observation to define the effective number of sequences in earthquake records of multiple sequences below.

In this section we propose that the effective number of acceleration sequences N_{ef} be defined based on the contribution of the sequence energy to the total energy of the ground acceleration. Let the total energy of the acceleration signal be described by Eq. (1) with $t = t_d$. The effective number of sequences is defined as the number of sequences that contribute by a minimum of a % to the total acceleration energy (a is a positive quantity to be specified). For instance, if a = 5, the earthquake records of Fig. 1(a) have two sequences while those of Fig. 1(b) have three sequences. The ratio of the PGA in each sequence to that of the entire record can be also used as a criterion for defining N_{ef}. This criterion, however, excludes important information, such as, the duration and the energy of each sequence. Similarly, the definition of the effective acceleration duration t_{ef} can also be introduced. Herein, t_{ef} is defined as the sum of individual effective durations of all sequences excluding the time intervals separating sequences. This duration reflects the actual duration of strong shaking of the ground. Based on this, the effective duration for the 2004 Niigata earthquake recorded at Nagaoka-shisho is about 50 s. This definition can be used in comparing the effective duration of ground shaking of ordinary records with records of multiple sequences. Note that the effective duration of repeated acceleration sequences can be compared with the effective duration or ordinary records using statistical analysis (see, e.g. Kempton and Stewart 2006).

To examine the frequency content and amplitude of repeated acceleration sequences, we use the short-time Fourier transform (STFT). Herein, the Fourier transform is estimated for snapshots or a sliding window of the original acceleration signal as follows

$$X(\omega, t) = \int_{-\infty}^{\infty} \ddot{x}(\tau)\; g(\tau - t) e^{-i\omega\tau} d\tau \tag{2}$$

where $X(\omega, t)$ is the Fourier transform of the acceleration at time t, $g(\tau)$ is a sliding rectangular window of unit intensity, ω is the circular frequency and $i = \sqrt{-1}$. Thus, for a fixed $t = t_j$, $X(\omega, t_j)$ represents the local spectral content of the ground acceleration as a function of the frequencies near t_j.

Fig. 6 depicts the STFT for the three records of the 2004 Niigata earthquake recorded at Nagaoka-shisho (NIG028) and those recorded at Koide (NIG020) (see Table 1). These plots reflect the non-stationarity of the acceleration sequences in time and frequency domains. Note that, the records of Fig. 6(a) have peak amplitudes at the frequency range (0-4) Hz, while those of Fig. 6(b) have peak amplitudes near 8.0 Hz. The frequency content of the ground accelerations is seen to be

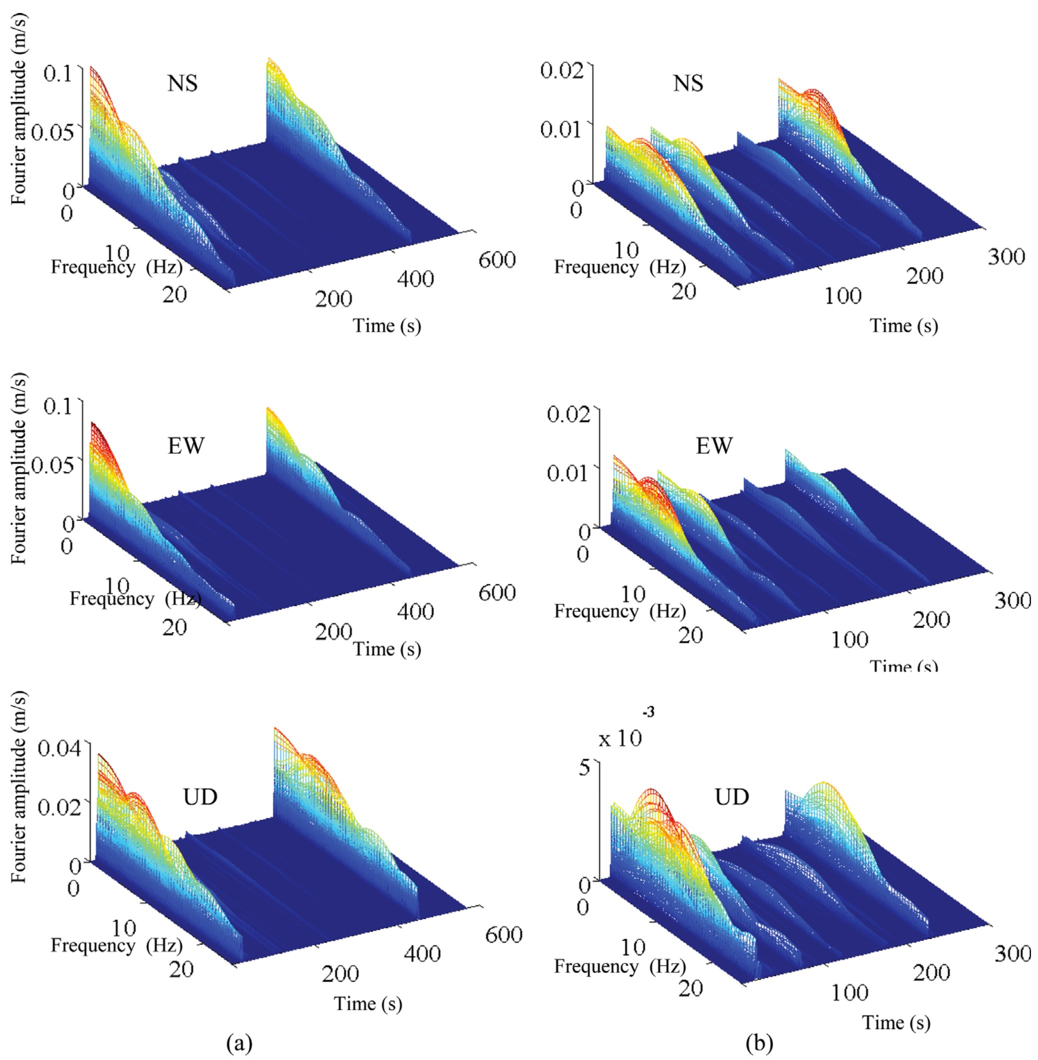

Fig. 6 Short-time Fourier amplitude spectra for repeated earthquake sequences: (a) 2004 Niigata earthquake at Nagaoka-shisho (NIG028) and (b) 2004 Niigata earthquake at Koide (NIG020)

about (0-30) Hz. The vertical accelerations are richer in frequency content compared to the horizontal components within the frequency range of (0-20) Hz. Note that, the STFT may lead to smooth spectra compared to the ordinary Fourier spectra when the length of the window function $g(\tau - t)$ is small. The next section examines the inelastic response of SDOF structures to repeated acceleration sequences.

3. Response, input energy and damage of SDOF inelastic structures to acceleration sequences

In this section, we examine the displacement response, the input and dissipated energies and the damage of SDOF inelastic structures to strong ground motions with repeated acceleration sequences. To do this, it is first noted that the equation of motion for the SDOF inelastic structure is given as (Chopra 2007)

$$m\ddot{u}(t) + c\dot{u}(t) + f_s(t) = -m\ddot{x}(t) \tag{3}$$

where m, c are the mass and the damping coefficient of the system, $f_s(t)$ is the nonlinear hysteretic restoring force, $u(t)$ is the displacement response, and dot indicates differentiation with respect to time. Note that, $u(t)$ is estimated using numerical integration techniques. The input energy per unit mass for the SDOF structure is given by (Takewaki 2004)

$$E_i(t) = -\int_0^t \ddot{x}(\tau)\ \dot{u}(\tau)d\tau \tag{4}$$

The kinetic and elastic strain energies are given, respectively, as

$$E_K(t) = \dot{u}^2(t)/2;\ \ E_S(t) = f_s^2(t)/(2k_0) \tag{5}$$

Herein, k_0 is the initial elastic stiffness. The hysteretic and damping energies are given as

$$E_H(t) = \int_0^t \dot{u}(\tau) f_s(\tau)d\tau - E_S(t);\ \ E_D(t) = \int_0^t c\ \dot{u}^2(\tau)d\tau \tag{6}$$

The literature on damage of structures during earthquakes and the use of damage indexes to quantify the associated damage level are vast. Khashaee presented an extensive review on this subject (Khashaee 2005). Herein, three expressions are adopted for quantifying the damage level for SDOF inelastic structures. The first damage index is given in terms of the maximum ductility demanded by the ground motion $\mu_{\max}$ (Powell and Allahabadi 1988)

$$DI_\mu = \frac{\mu_{\max} - 1}{\mu_u - 1} \tag{7}$$

Herein μ_u is the ultimate ductility capacity of the structure under monotonic loading determinable from experimental tests. The second damage index is given in terms of the normalized hysteretic energy demanded by the earthquake (Cosenza *et al*. 1993)

$$DI_H = \frac{E_H/(f_y u_y)}{\mu_u - 1} \tag{8}$$

where E_H, f_y, u_y are the hysteretic energy demand, the yield strength and the yield displacement, respectively. Park and coworkers expressed damage as a linear combination of the maximum ductility and the hysteretic energy (Park and Ang 1985, Park *et al.* 1987)

$$DI_{PA} = \frac{\mu_{\max}}{\mu_u} + \beta\frac{E_H/(f_y u_y)}{\mu_u} \tag{9}$$

where β is a positive constant that weighs cyclic loading effects on structural damage (typically β ranges between 0 and 0.30). The quantities μ_{max}, E_H depend on the loading history while β, μ_u, f_y are determined from experimental tests. Note that, the first damage index does not account for energy dissipation while the second damage index is dependent on the hysteretic energy. The third damage index accounts for effects from maximum ductility and cyclic loadings. This damage index, although has some limitations, it has been widely used by many researchers due to its simplicity and extensive experimental calibrations of structures during earthquakes (Moustafa 2011). The structure's damage state is defined as (a) repairable damage ($DI_{PA} < 0.40$), (2) damaged beyond repair ($0.40 \le DI_{PA} < 1.0$) and (c) total collapse ($DI_{PA} \ge 1.0$) (Park and Ang 1985).

To examine the effect of the acceleration sequences on the structural inelastic response, we estimate the response of an elastic-perfectly plastic SDOF structure of initial period = 2.0 s to the NS acceleration of the 2004 Niigata earthquake recorded at Nagaoka-shisho. A viscous damping of 0.03 damping ratio is adopted. The yield strength and initial stiffness are taken as 5×10^3 N and 1.49×10^5 N/m, respectively. These parameters are changed later to examine their influence on the structure's response. The dynamic analysis is carried out using the Newmark-β linear acceleration method with time step = 0.005 s.

Fig. 7 depicts the displacement, the input, the hysteretic and the damping energies, the force-displacement hysteretic loops and the damage indexes (Eqs. (7)-(9)). The displacement response reveals that each acceleration sequence drives the structure to a new equilibrium position (see Fig.

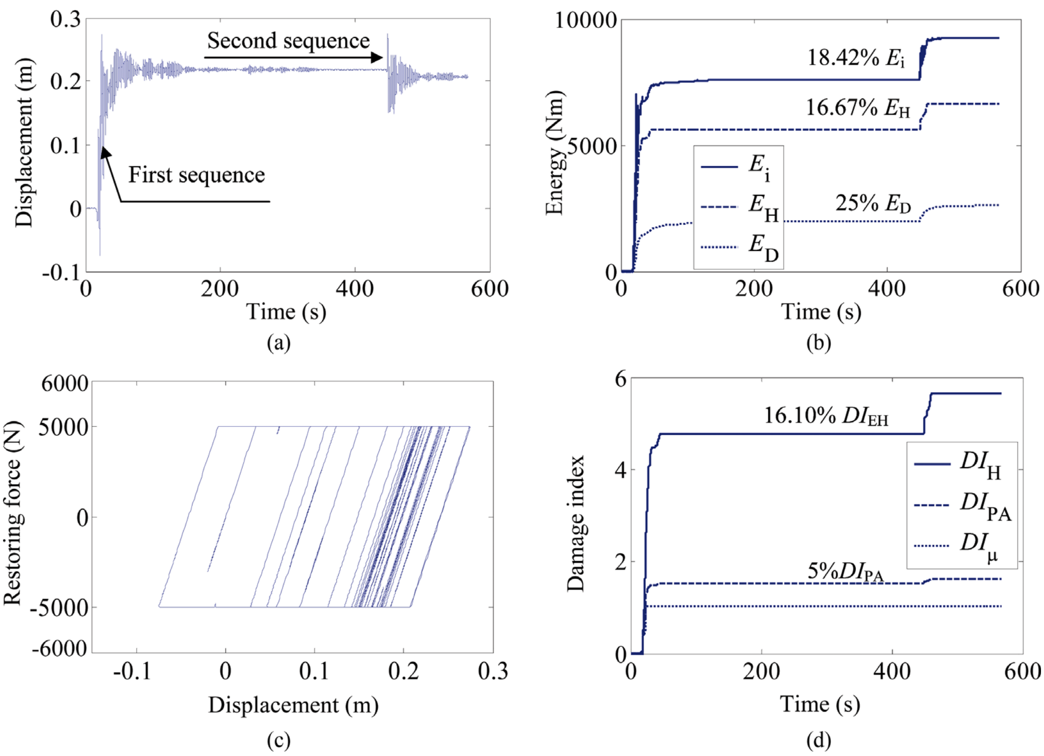

Fig. 7 Time-variation of input energy and response quantities for elastic-plastic structure ($f_y = 5\times10^3$ N, T_0 = 2.0 s) under 2004 Niigata NS record (Nagaoka-shisho): (a) Displacement response, (b) Input, hysteretic and damping energies, (c) Force-displacement hysteretic loops and (d) Damage indexes

7(a)) and that a significant permanent deformation remains at the end of the ground shaking. The second sequence slightly increases the maximum displacement (secondary sequences of other records increase the maximum displacement by up to 20%) but has substantial effect on the input, hysteretic and damping energies (see Fig. 7(b)). It is seen that most of the input energy (about 82%) results from the first sequence. However, the maximum displacement response is attained during the second sequence.

The influence of the second sequence on the force-displacement hysteretic loops and on the hysteretic energy demand for two different yield strength values are shown in Fig. 8. The second sequence causes more yielding to the structure (Fig. 8 and Table 2). The force-displacement

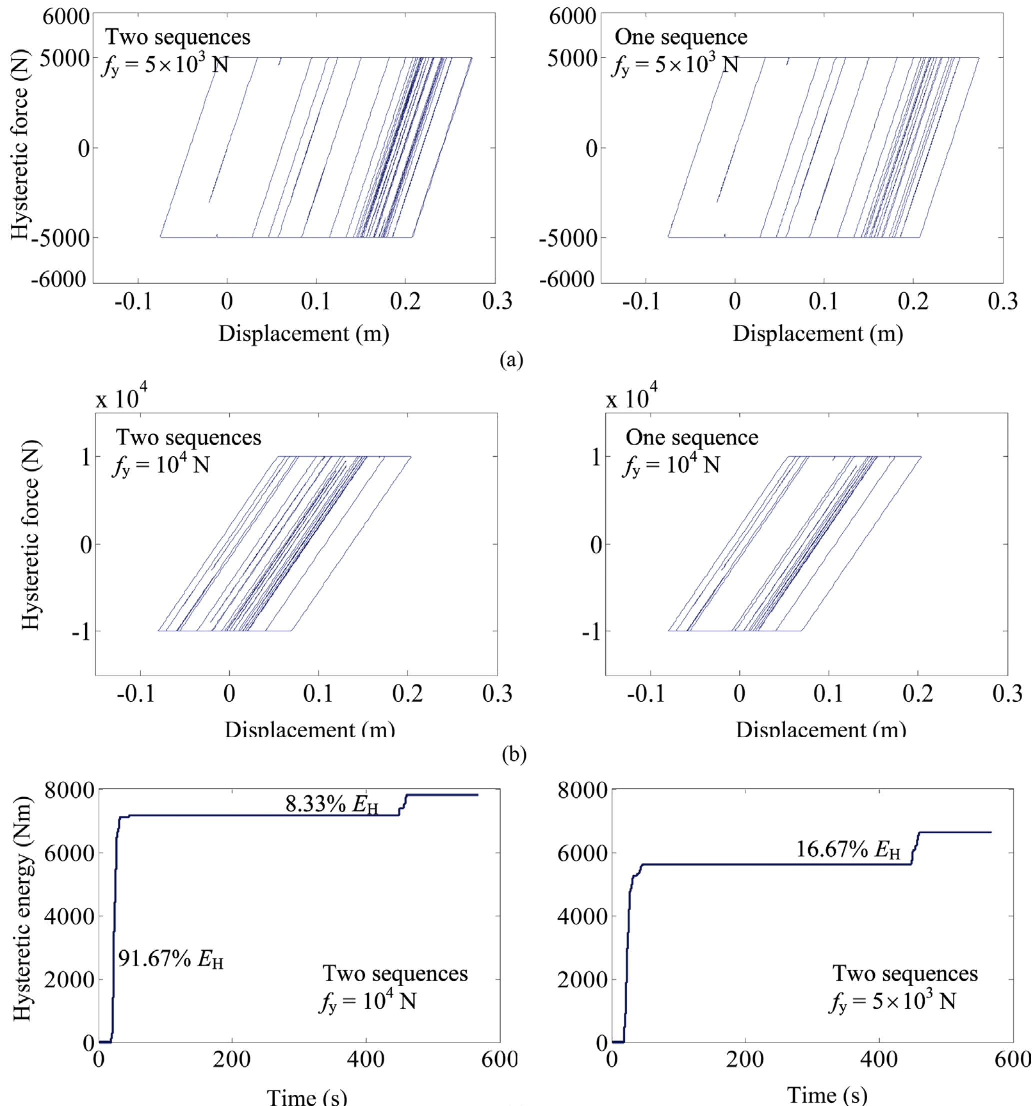

Fig. 8 Influence of number of sequences and yield strength on the hysteretic energy and hysteretic loops for elastic-plastic structure (T_0 = 2.0 s) under 2004 Niigata NS record (Nagaoka-shisho)

Table 2 Influence of secondary acceleration sequences on the response quantities of SDOF elastic-plastic structure (T_0 = 2.0 s)

Yield strength f_y	First acceleration sequence only								First and second acceleration sequences							
	$DF_{\max}$	$E_{H\max}$ (Nm)	$E_{D\max}$ (Nm)	N_y	DI_{PA}	DI_H	DI_μ	$\|u_p\|$ (m)	$DF_{\max}$	$E_{H\max}$ (Nm)	$E_{D\max}$ (Nm)	N_y	DI_{PA}	DI_H	DI_μ	$\|u_p\|$ (m)
5×10^3 (N)	8.16	5608	1908	1447	1.52	4.78	1.02	0.19	8.19	6643	2615	1947	1.62	5.66	1.03	0.21
1×10^4 (N)	3.01	7157	3107	723	0.54	1.52	0.29	0.08	3.04	7821	4270	893	0.55	1.67	0.29	0.04
2×10^4 (N)	1.82	8220	5654	326	0.27	0.44	0.12	0.03	1.82	8220	7440	326	0.27	0.44	0.12	0.02

T_0 = initial natural period, $DF_{\max}$ = maximum ductility, $E_{H\max}$ = maximum hysteretic energy, $E_{D\max}$ = maximum damping energy, N_y = number of yield reversals, u_p = permanent deformation, DI_{PA}, DI_H, DI_μ = damage indexes (Eqs. (7)-(9))

hysteretic loops, the hysteretic energy and damping energy are significantly influenced by the second sequence. For instance, E_H increases by about 17% and E_D increases by about 25% due to the second sequence. Furthermore, the input energy and the displacement response were seen to be larger for the lower yield strength. This observation is confirmed by the hysteretic loops shown in Figs. 8(a) and (b). The structure with higher yield strength has small damage indexes while that with lower yield strength has large damage indexes. Thus, DI_{PA} = 1.62 (total collapse) for $f_y = 5 \times 10^3$ N, DI_{PA} = 0.55 (damaged beyond repair) for $f_y = 1 \times 10^4$ N and DI_{PA} = 0.27 (repairable damage) for $f_y = 2 \times 10^4$ N ($\beta = 0.12$, $\mu_u = 8.0$). The associated ductility demands (8.19, 3.04 and 1.82) correspond to high, moderate and low ductility level, respectively. The effect of the second sequence on the Park and Ang damage index is small (about 5%). However, the damage index of Eq. (8) increases by about 16% due to the second sequence. When the yield strength decreases from 10^4 N to 5×10^3 N, the maximum ductility demand increases 2.7 times, the maximum hysteretic energy decreases by about 70%, the number of yield points doubles, the permanent plastic deformation increases 5 times, DI_{PA} increases 2.9 times (the damage state changes from damaged beyond repair to total collapse) and DI_μ increases about 3.5 times (see Table 2). Hence, the structural response depends on the yield parameters. The structural response under the earthquake records listed in Table 1 has been computed and the general feature was found to be the same.

To examine the influence of the structure's initial natural period on the inelastic response to different acceleration sequences, we estimate the response of three inelastic structures with initial natural periods $T_0 = 0.3$, 1.0 and 3.0 s under the horizontal acceleration (H_1) of the earthquake records in Table 1. These natural periods represent typical structures of short-period (< 0.5 s), medium-period (0.5-1.5 s) and long-period (> 1.5 s). We determine also the same response quantities for the two ordinary records. Elastic-plastic and bilinear inelastic force-deformation laws have been considered ($f_y = 1 \times 10^4$ N and $\zeta = 0.03$).

The numerical results of these analyses are presented in Fig. 9 and Table 3. Fig. 9 shows the time variation of the input energy and the damage index DI_{PA} for SDOF elastic-plastic structures to two earthquake records with two sequences and for the ordinary records. The input energy and the damage indexes are seen to depend on the structure's fundamental period and the dominant period and intensity of the input acceleration. For instance, the NS component of the 2004 Niigata earthquake (NIG028) produces the maximum input energy and the maximum damage index for the structures with short- and medium-periods. The NS record of the 2004 Niigata earthquake (NIG020) results in the least input energy and damage index. The 1940 El Centro record provides the largest

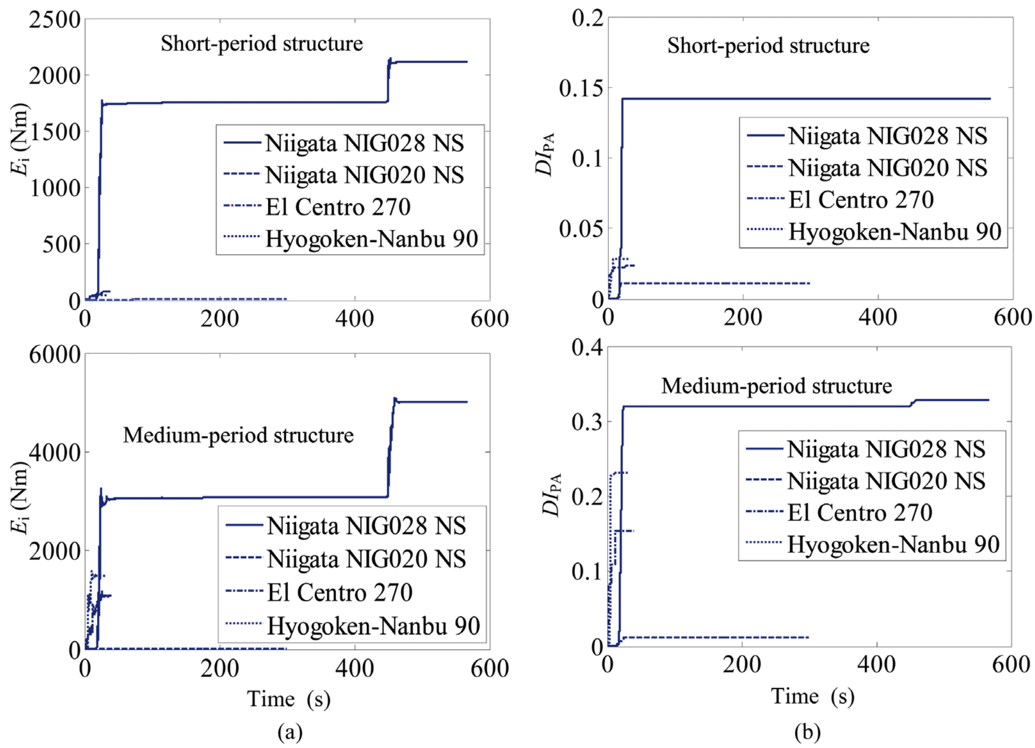

Fig. 9 Time-variation of input energy and Park and Ang damage index for elastic-plastic structures under different earthquake inputs: (a) Input energy and (b) Damage index

input energy and damage indexes for the structure with long-period (this record has large amplitude near T_0 = 3.0 s). The structures with short- and medium-periods are either damaged with repairable damage ($DI_{PA} < 0.40$) or behave elastically (see Fig. 9 and Table 3). The long-period structure behaves elastically under the 2004 Niigata (NIG020) record and is damaged beyond repair ($DI_{PA} >$ 0.40) under other records. Note that, the influence of the repeated sequences is more obvious in the plots of the input energy to the structure compared to the plots of the damage index (Fig. 9). Accordingly, it can be concluded that, the ground acceleration with multiple sequences does not always produce the maximum response and/or damage in the structure. In other words, the structural inelastic response depends on the structure's initial natural period, the yield parameters and the associated dominant period and intensity of the ground motion. Tables 1 and 3 summarize the intensity (Eq. (1)) and the average frequency content (f_0-f_c) of the ground acceleration (the frequency range that contains 90% of the acceleration intensity) (Moustafa and Takewaki 2010a,b). The numerical values of these parameters confirm that the structure's response depends on the characteristics of the input acceleration and the structure's properties.

To compare the structural responses of elastic-plastic and bilinear structures, we consider two SDOF systems of initial natural period = 1.0 s, initial stiffness = 1.49×10^5 N/m, viscous damping ratio = 0.03 and yield strength in tension and compression = 5×10^3 and -5×10^3 N, respectively. The strain-hardening ratio of the bilinear structure is taken as 0.05. The two structures are assumed to be driven by the horizontal acceleration H_1 (see Table 1) of the Iwate-Miyagi earthquake with PGA = 1.0 g. The responses for the two structures are shown in Fig. 10. The maximum input

Table 3 Response and damage parameters for short-, medium- and long-period SDOF elastic-plastic structures to ground motion with repeated sequences (H_1 acceleration component in Table 1)

Input record (f_0-f_c) Hz	Short-period structure (T_0 = 0.30 s)						Medium-period structure (T_0 = 1.0 s)						Long-period structure (T_0 = 3.0 s)					
	μ_{max}	E_{max} (Nm)	N_y	$\lvert u_p\rvert$ (m)	DI_{PA}	DL	μ_{max}	E_{max} (Nm)	N_y	$\lvert u_p\rvert$ (m)	DI_{PA}	DL	μ_{max}	E_{max} (Nm)	N_y	$\lvert u_p\rvert$ (m)	DI_{PA}	DL
Helena aft. (0-22)	1.44	838.65	20	0.08	0.15	RD	0.44	71.68	0	0.01	0.04	ND	0.05	1.30	0	0	0.01	ND
San Francisco (0-15)	0.20	55.06	0	0.01	0.03	ND	0.11	9.05	0	0	0.01	ND	0.08	5.68	0	0	0.01	ND
San Fernando (0-30)	0.10	50.84	0	0	0.01	ND	0.06	9.82	0	0	0	ND	0.11	9.40	0	0	0.01	ND
Victoria (0-19)	2.28	7944.5	777	0	0.30	RD	0.55	504.91	0	0	0.06	ND	0.27	70.52	0	0	0.03	ND
New Zealand (0-25)	0.06	28.53	0	0	0.01	ND	0.14	17.73	0	0	0.01	ND	0.06	5.16	0	0	0.01	ND
Katsurao (0-35)	0.03	10.63	0	0	0	ND	0.03	3.41	0	0	0	ND	0.07	4.62	0	0	0.01	ND
Kocaeli (0-10)	6.58	21183	1562	0.33	0.94	TC	1.66	2180.7	73	0.04	0.17	RD	0.23	87.22	0	0	0.02	ND
Chi-Chi (0-12)	2.51	4722.4	245	0.09	0.28	RD	2.05	4794	209	0.06	0.24	RD	0.59	609.08	0	0	0.06	ND
Chi-Chi (0-20)	0.65	489.65	0	0	0.07	ND	0.78	628.24	0	0	0.08	ND	0.29	94.9	0	0	0.03	ND
Bhuj (0-25)	0.92	787.68	0	0	0.09	ND	0.70	480.8	0	0	0.07	RD	0.13	29.41	0	0	0.01	ND
Niigata (0-20)	3.23	20393	362	0.07	0.51	DBR	2.72	15405	237	0.05	0.44	DBR	1.16	1201.8	3	0.01	0.11	ND
Niigata (0-25)	2.34	15089	905	0.05	0.38	RD	2.29	6474.4	198	0.08	0.28	RD	0.76	1590.2	0	0	0.08	ND
Niigata (0-20)	1.10	1725.9	10	0	0.11	RD	0.88	920.08	0	0	0.09	ND	0.15	71.65	0	0	0.02	ND
Niigata (0-32)	0.12	15.31	0	0	0.01	ND	0.08	9.26	0	0	0.01	ND	0.03	1.36	0	0	0.01	ND
Niigata (0-21)	1.53	1921.7	32	0.04	0.16	RD	0.78	655.58	0	0	0.08	ND	0.55	491.44	0	0	0.06	ND
Niigata (0-30)	0.17	43.07	0	0	0.017	ND	0.08	16.87	0	0	0.01	ND	0.11	10.72	0	0	0.01	ND
Niigata (0-23)	2.04	3032.2	59	0.06	0.22	RD	1.41	1835.7	18	0.03	0.15	RD	0.79	485.2	0	0	0.08	ND
Honshu (0-34)	0.17	60.83	0	0	0.02	ND	0.27	90.92	0	0	0.03	ND	0.13	32.37	0	0	0.01	ND
Niigata-ken (0-26)	0.11	27.93	0	0	0.01	ND	0.14	32.45	0	0	0.01	ND	0.05	3.17	0	0	0.01	ND
Iwate-Miyagi (0-32)	0.28	394.87	0	0	0.03	ND	0.29	114.65	0	0	0.03	ND	0.17	20.82	0	0	0.02	ND
El Centro (0-18)	3.11	4980.3	121	0.14	0.35	RD	1.44	2333.6	44	0.01	0.16	RD	0.27	112.12	0	0	0.03	ND
Hyog.-Nanbu (0-12)	2.30	8762	168	0.09	0.32	RD	3.67	5690.0	138	0.12	0.43	DBR	0.27	65.30	0	0	0.03	ND

T_0 = initial natural period, μ_{max} = maximum ductility, $E_{H\max}$ = maximum hysteretic energy, N_y = number of yield reversals, u_p = permanent deformation, DI_{PA}, DI_μ = damage indexes (Eqs. (7)-(9)), DL = damage level, ND = non-damaged (linear behavior), RD = repairable damage, DBR = damaged beyond repair, TC = total collapse.

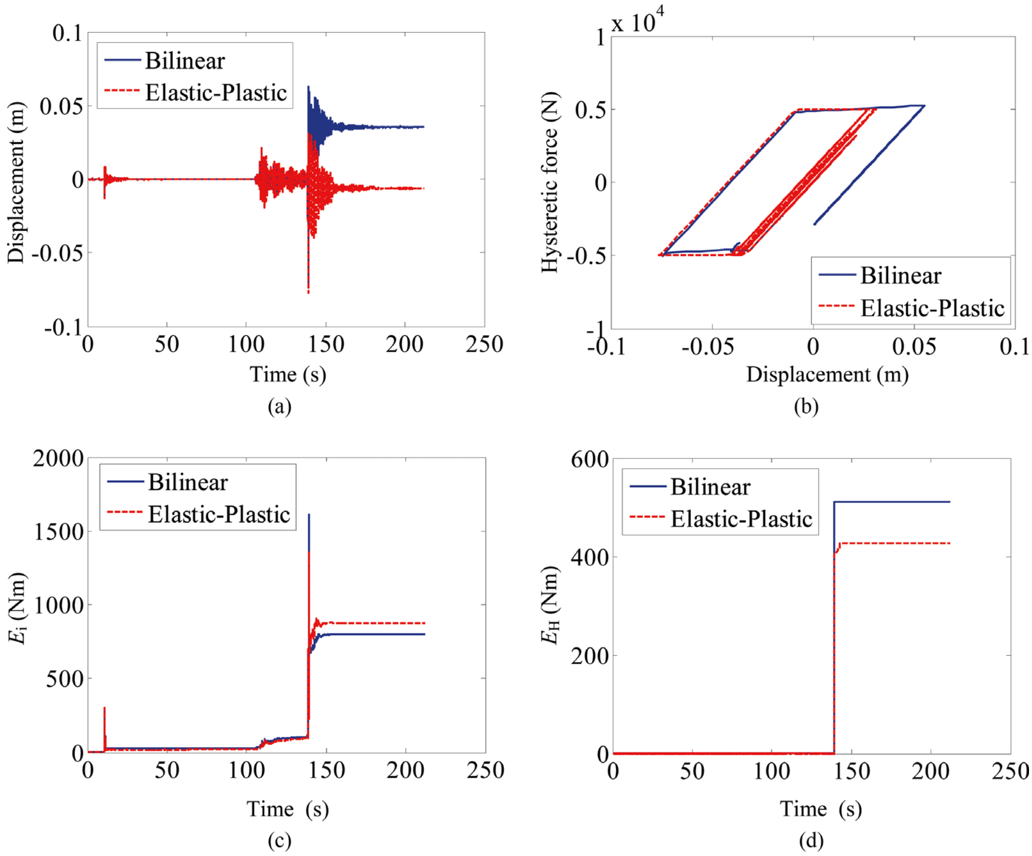

Fig. 10 Response of elastic-plastic and bilinear inelastic SDOF structures to the horizontal acceleration H_1 of the 2007 Iwate-Miyagi earthquake: (a) Displacement, (b) Hysteretic loops, (c) Input energy and (d) Hysteretic energy

energy to the elastic-plastic structure is seen to be slightly smaller than that for the bilinear inelastic structure (Fig. 10(c)). However, the maximum displacement of the elastic-plastic structure is higher than that for the bilinear structure by about 10% (Fig. 10(a)). Additionally, the elastic-plastic structure is seen to yield more frequently ($Ny = 33$) than the bilinear structure ($Ny = 8$) (Fig. 10(b)). The maximum hysteretic energy dissipated by the bilinear structure is 16% higher than the hysteretic energy dissipated by the elastic-plastic structure. These results reveal that the elastic-plastic structure is more vulnerable to the acceleration sequences compared with the bilinear structure (see e.g. Amadio *et al.* 2003).

4. Conclusions

Multiple sequences of ground accelerations separated by short time-intervals have been observed in Japan, Mexico, Italy, Turkey, Peru, California and other regions of the world. This paper investigates the general features of this class of ground motion. Specifically, the number, the duration, PGA and the energy of the individual sequences and the gross properties of the entire record, such as, the duration, PGA, the Fourier amplitude and the frequency content, the local soil condition, and the site-source distance have been studied. The definitions of the effective number of sequences and the effective duration of recorded acceleration sequences have also been introduced. The two horizontal components and the vertical accelerations of 20 strong-motion earthquakes have been used in the numerical investigation. These records are measured in seven different countries and cover a variety of earthquake magnitude, duration, site-source distance, peak ground acceleration and local soil condition. Note that the parameters of the repeated acceleration sequences, such as, the total duration and the effective number of sequences depend on the acceleration records adopted. In this context, it may be emphasized that this study does not provide statistical analyses for acceleration sequences but highlights the features of acceleration sequences and investigates the associated structural inelastic response.

The individual sequences of multiple acceleration sequences are seen to have short duration, sharp build up, short strong-phase and sudden decay. These characteristics should be considered in simulating acceleration sequences. In this study, the general characteristics of the ground motion of multiple sequences that are commonly relevant to engineers have been studied. The seismological properties and the modeling of acceleration sequences, using predictive and engineering models, including the discontinuity of the released energy at the source and the associated attenuation due to path and local soil effects still need to be studied.

The structural response under recorded acceleration sequences has been studied. Each sequence was seen to drive the structure into a new equilibrium position. Secondary sequences were seen to increase the ductility demand, the number of yield points, and the input, hysteretic and damping energies. Their influences on damage indexes that are based on maximum ductility are small, but have substantial effect on damage indexes that are based on hysteretic energy demand. In this paper, elastic-plastic and bilinear SDOF inelastic structures have been studied. It is also of interest to examine the structural behavior of inelastic MDOF structures with degrading stiffness and/or strength which can describe the formation of plastic hinges and the time-dependent damage of the structure.

Acknowledgements

This work is supported by research funds from the Japanese Society for the Promotion of Science under Grant No. JSPS-P-08073. The support is gratefully acknowledged. The authors are also thankful to the K-Net, KiK-Net, the PEER center and the COSMOS center for providing the ground motion records used in this study.

References

Amadio, C., Fragiacomo, M. and Rajgelj, S. (2003), “The effects of repeated earthquake ground motions on the non-linear response of SDOF systems”, *Earthq. Eng. Struct. D.*, **32**(2), 291-308.

Architecture Institute of Japan (2005), *Recommendations for loads on buildings*, Tokyo.

Arias, A. (1970), *A measure of earthquake intensity: seismic design of nuclear power plants*, Cambridge, MA: MIT press, 438-468.

Bray, J.D. and Rodriguez-Marek, A. (2004), “Characterization of forward-directivity ground motions in the nearfault region”, *Soil. Dyn. Earthq. Eng.*, **24**(11), 815-828.

Chopra, A.K. (2007), *Dynamics of structures*, 3rd edition, Prentice Hall, NJ.
Cosenza, C., Manfredi, G. and Ramasco, R. (1993), "The use of damage functionals in earthquake engineering: a comparison between different methods", *Earthq. Eng. Struct. D*., **22**(10), 855-868.
COSMOS (2009), *Consortium organizations for strong-motion observation systems*, http://db.cosmos-eq.org/scripts/default.plx
Das, S., Gupta, V.K. and Srimahavishnu, V. (2007), "Damage-based design with no repair for multiple events and its sensitivity to seismicity model", *Earthq. Eng. Struct. D*., **36**(3), 307-325.
Elnashai, A., Bommer, J.J. and Martinez-Pereira, A. (1998), "Engineering implications of strong-motion records from recent earthquakes", *Proceedings of 11th European Conference on Earthquake Engineering*, Paris, CD-ROM.
European Committee for Standardization (2003), *Eurocode 8: Design of structures for earthquake resistance*, Brussels.
Fragiacomo, M., Amadio, C. and Macorini, L. (2004), "Seismic response of steel frames under repeated earthquake ground motions", *Eng. Struct*., **26**(13), 2021-2035.
Hatzigeorgiou, G.D. and Beskos, D.E. (2009), "Inelastic displacement ratios for SDOF structures subjected to repeated earthquakes", *Eng. Struct*., **31**(11), 2744-2755.
Hatzigeorgiou, G.D. (2010a), "Ductility demand spectra for multiple near- and far-fault earthquakes", *Soil Dyn. Earthq. Eng*., **30**(4), 170-183.
Hatzigeorgiou, G.D. (2010b), "Behavior factors for nonlinear structures subjected to multiple near-fault earthquakes", *Comput. Struct*., **88**(5-6), 309-321.
International Building Code (2009), *International code council*, Inc., First printing, IL.
Kalkan, E. and Kunnath, S.K. (2006), "Effects of fling step and forward directivity on seismic response of buildings", *Earthq. Spectra*, **22**(2), 367-390.
Kempton, J.J. and Stewart, J.P. (2006), "Prediction equations for significant duration of earthquake ground motions considering site and near-source effects", *Earthq. Spectra*, **22**(4), 985-1014.
Khashaee, P. (2005), "Damage-based seismic design of structures", *Earthq. Spectra*, **21**(2), 371-387.
Kiban-Kyoshin Network (2009), *National research institute for earth science and disaster prevention*, http://www.kik.bosai.go.jp/.
Krawinkler, H., Alavi, B. and Zareian, F. (2005), *Imapct of near-fault pulses on engineering design: Directions in strong motion instrumentation*, Polat Gulkan and John G. Anderson (eds), Springer, Dordrecht.
Kyoshin-Network (2009), *National research institute for earth science and disaster prevention*, http://www.knet.bosai.go.jp/.
Li, Q. and Ellingwood, B.R. (2007), "Performance evaluation and damage assessment of steel frame buildings under main shock–aftershock earthquake sequences", *Earthq. Eng. Struct. D*., **36**(3), 405-427.
Moustafa, A. (2011), "Damage-based design earthquake loads for SDOF inelastic structures", *J. Struct. Eng.-ASCE*, **137**(3), 456-467.
Moustafa, A. and Takewaki, I. (2010a), "Deterministic and probabilistic representation of near-field pulse-like ground motion", *Soil Dyn. Earthq. Eng*., **30**(5), 412-422.
Moustafa, A. and Takewaki, I. (2010b), "Characterization and modeling of near-fault pulse-like strong ground motion via damage-based critical excitation method", *Struct. Eng. Mech*., **34**(6), 755-778.
Nour, S.D., Barbuta, M. and Mihul, A. (1992), "Analysis of the behaviour of some historical consolidated buildings made of brick masonry to repeated earthquakes", *Proceedings of the 10th World Conference on Earthquake Engineering*, Balkema, Rotterdam, 5327-5331.
Park, Y.J. and Ang, A.H.S. (1985), "Mechanistic seismic damage model for reinforced concrete", *J. Struct. Eng.-ASCE*, **111**(4), 722-739.
Park, Y.J., Ang, A.H.S. and Wen, Y.K. (1987), "Damage-limiting aseismic design of buildings", *Earthq. Spectra*, **3**(1), 1-26.
PEER (2009), *Pacific earthquake engineering research center*, http://peer.berkeley.edu/smcat/search.html.
Powell, G.H. and Allahabadi, R. (1988), "Seismic damage predictions by deterministic methods: concepts and procedures", *Earthq. Eng. Struct. D*., **16**(5), 719-734.
Takewaki, I. (2004), "Bound of earthquake input energy", *J. Struct. Eng.-ASCE*, **130**(9), 1289-1297.
Trifunac, M.D. and Brady, A.G. (1975), "A study on the duration of strong earthquake ground motion", *B. Seismol. Soc. Am*., **65**(3), 581-626.

CC